measurements, the Pioneer Venus Orbiter probes provided measurements of the total solar EUV flux at Venus between 1978 and 1992 based on the amplitude of the photo emission current from one of the collectors. This ancillary use of Langmuir probes was reported by Brace et al. (1988) and will not be discussed again here.

Each of these missions provided useful lessons. Perhaps the key lesson is that the accuracy of the measurements is determined less by the theory of the method than by shortcomings in design and implementation. We found that most measurement errors arose from one or more of the following; the type of collector surface material used, failure to avoid surface contamination or to provide for inflight cleaning of the collector, failure to place the collector an adequate distance from the spacecraft and from various appendages that might interfere with its access to undisturbed plasma, failure to design the electronics to adequately resolve those portions of the volt-ampere curves that contain the desired geophysical information and, finally, failure to assure that the spacecraft is able to serve as a stable potential reference for the measurements. The purpose of this paper is to discuss these sources of error and indicate how they can be reduced to an acceptable level.

OVERVIEW OF THE METHOD

The LP technique involves measuring the volt-ampere characteristics of one or more bare metal collectors mounted on booms. A typical experimental setup is shown conceptually in Figure 1 which shows a radial probe and an axial probe on a spacecraft having an internal momentum wheel that allows it to operate in either spinning or despun modes, as in the AE and DE-2 missions. The radial probe is oriented perpendicular to the spin axis and is mounted on a deployable boom which is long enough to reach the undisturbed plasma beyond the spacecraft ion sheath. A length of 30 to 100 cm is adequate for most ionosphere applications. (An outer plasmasphere mission would require a longer boom to accommodate the larger Debye shielding distances.) The radial probe is perpendicular to the velocity vector when the spacecraft is despun, thus permitting continuous measurements at the preferred angle of attack. In the spin mode, the radial probe makes its most useful measurements as it passes through 90^{o} angle of attack twice per spin. For reliability, the axial probe is mounted on a boom that is short enough to avoid the need to stow it for launch and deploy it in orbit. If the spin axis is perpendicular to the orbit plane, as in the AE and DE missions, the axial probe remains at 90^{o} angle of attack whether or not the spacecraft is spinning. This approach essentially eliminates spin modulation and allows continuous measurements that the radial probe cannot provide when the spacecraft is spinning. The axial probe is sometimes operated at a fixed potential to provide high resolution measurements of N_e or N_i, but it can also be

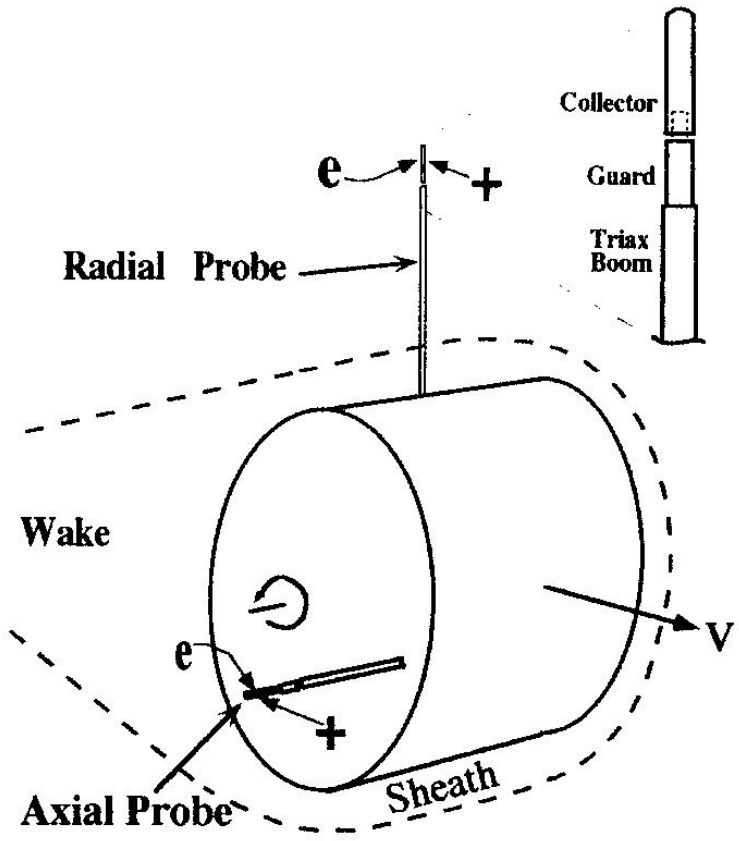

Figure 1. A typical LP arrangement. Two cylindrical probes are mounted on solid triaxial booms. The radial probe is oriented perpendicular to the spin axis and the axial probe is parallel to the spin axis. Both probes are oriented perpendicular to the velocity vector when the spacecraft is despun.

commanded to a sweeping mode which measures T_e and V_S in the event of damage, failure to deploy, or contamination of the radial probe. The two probes can time-share the same electrometer if simultaneous operation and electronic redundancy are not required. Both probes have a guard electrode that is driven at the same potential as the collector to reduce electrical end effects.

Figure 2 illustrates the measurement technique. Volt-ampere characteristics are obtained by repeatedly sweeping the collector voltage, V_a, with respect to the spacecraft potential, V_S, while measuring the net current, I, which is the sum of the ion current, I_i, and the electron current, I_e. The electronics contains an electrometer, a sweep voltage generator and adaptive circuitry that adjusts the gain and sweep amplitude to track the changing density and temperature. The electrometer output is digitized and recorded for eventual telemetry to a ground station along with the necessary information on electrometer gain and sweep voltage amplitude. The adaptive function, first described by Brace et al. (1973), employs hard-wired logic circuitry which examines the electrometer output during each voltage sweep to determine the gain and sweep voltage

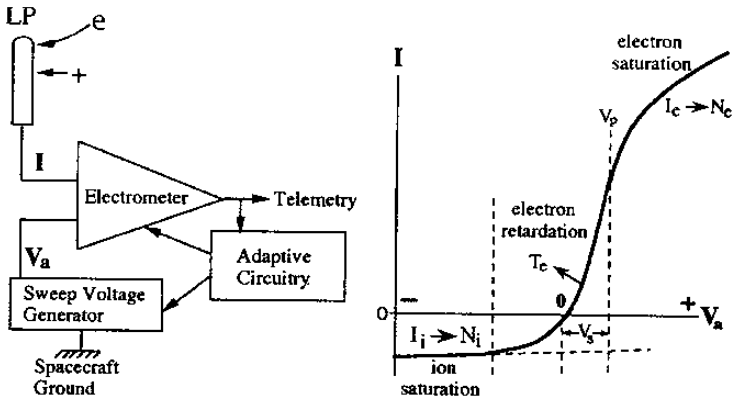

Figure 2. Block diagram of the electronics and a typical volt-ampere curve. N_i, N_e and T_e are derived from different parts of the curve, as discussed in the text. Adaptive circuitry adjusts the electrometer gain and sweep voltage amplitude to "frame" the volt-ampere curves for telemetry over a wide range of N_i and T_e variation. The sweep voltage, V_a, is applied with respect to the spacecraft floating potential, V_s.

settings required to achieve a so called "ideal curve" on the subsequent sweep. This adaptive operation accomplishes two goals; (1) it focuses the limited telemetry bit rate on just the portion of the curve needed to derive N_e, N_i, and T_e, and (2) it generates gain and amplitude settings that can be telemetered at low bit rate to serve as inflight measurements of N_i and T_e. More details are given in the Implementation section.

The theoretical volt-ampere curve shown at the right of Figure 2 illustrates how the measurements are deduced from the curves. The ion current scale has been expanded by a factor of 5 or so for illustration purposes. According to LP theory (Mott-Smith and Langmuir, 1926) the amplitude of the electron current, I_e, is proportional to N_e, and the amplitude of the ion current, I_i, is proportional to N_i. T_e determines the width of the electron retardation region. The measured current, I, is the sum of I_i and I_e. V_a is the sweep voltage that is applied to the probe with respect to the spacecraft potential, V_S. In the ionosphere, V_S assumes an equilibrium potential that is 3 or 4 kT_e negative with respect to the plasma potential, V_p. In the rest of this paper we discuss the theoretical basis for the LP measurements and some of the major factors to consider when implementing an experiment.

THEORY OF THE METHOD

There is no general theory that applies to all Langmuir probe geometries, plasma conditions, spacecraft velocities and probe orientations. Therefore, probes are usually designed for special limiting cases; such as orbital-motion-limited collection or sheath-area-limited collection (Langmuir and Mott-Smith, 1924, Mott-Smith and Langmuir, 1926). To remain orbital-limited the probe radius must be small compared with the thickness of the sheath that surrounds it, while the radius of a sheath-area-limited probe must be large compared to the sheath thickness. The equations for these limiting cases are simple enough to be incorporated easily into the data processing codes that are designed to process the tens of millions of volt-ampere curves that are recovered during a satellite mission.

The "Dumbbell" probes used on early rockets by Boggess et al. (1959) and Spencer et al. (1965) are examples of sheath-area-limited probes. These probes were too large (radius ~10 cm) for satellite use, and they would have to have been even larger to remain sheath-area-limited at the low densities of the upper F-region and plasmasphere. Therefore satellite Langmuir probes have usually been made small enough to remain orbital-motion-limited. The probe can be either spherical or cylindrical. We have adopted the cylindrical geometry because the probe radius can be made small enough to remain orbital-motion-limited at very high ionosphere densities, while its length can be made great enough to collect a measurable current at very low densities. In the early missions referenced above, the collector was a long, thin stainless steel wire (23 x 0.056 cm) whose low mass made it easily boom-mounted and whose strength made it rugged enough to withstand the rigors of the launch environment. The probes used in later missions were shorter and larger in diameter (5 x 0.4 cm) to reduce the voltage induced in the collector as it cuts the geomagnetic field at high velocity, an effect that will be discussed in detail later.

The first step in the analysis of a volt-ampere curve like the one shown in Figure 2 is to employ the LP current equations to fit the ion saturation and electron retardation regions to obtain N_i, T_e and V_p. V_p is taken either as the last point in the retardation region that provides a good fit to the exponential, or it may be taken as the inflection point between the electron retardation and saturation region. All potentials referred to in the Langmuir probe equations are measured with respect to this point. Once V_p has been determined, the electron saturation region is fitted to obtain N_e. The appropriate equations for an orbital-motion-limited cylinder are discussed below.

The N_e Measurements

When the collector radius is small compared to the Debye length, which determines the thickness of the ion sheath, the electron collection is said to be orbital-motion-limited (Mott-Smith and Langmuir, 1926). The equation for the electron saturation current is given by

$$I_e = N_e A e 2\pi^{-1/2} (kT_e/2\pi m_e)^{1/2} (1+eV/kT_e)^{1/2} \qquad (1)$$

where:

- A = probe surface area
- e = electron charge
- k = Boltzmann constant
- m_e = electron mass
- V = probe potential relative to V_p

By inspection, equation 1 has two terms, involving 1 and eV/kT_e, respectively. The first term represents the random electron flux that strikes an uncharged cylindrical probe simply because it is physically there. The second term accounts for the additional current that is collected when the probe is driven positive with respect to V_p. I_e increases as the square root of eV/kT_e in this region.

An advantage of the cylindrical geometry can be appreciated by further inspection of equation 1. Note that the electron saturation current becomes essentially independent of T_e at higher voltages ($eV/kT_e >> 1$) where the kT_e terms cancel. This feature makes it possible to measure N_e without knowledge of T_e. Thus long cylindrical probes have the practical advantage that they can be operated at a fixed positive potential to make continuous, high precision, measurements of N_e without interruption to obtain volt-ampere curves to determine T_e. Since the spatial resolution is limited only by the electrometer frequency response and the available telemetry rate, measurements made with a fixed V_a can resolve the small scale structure associated with ionospheric irregularities and plasma bubbles.

Because Equation 1 represents a simple asymptotic form of the more general equation for orbital-motion-limited collection by an infinitely long probe its use overestimates N_e. The shorter probes used on AE-C, DE-2 and PVO tended to have large "end effects", a term that refers to the tendency of the far end of the probe to collect electrons more efficiently than the rest of the probe. (The guard electrode reduces the end effect at the near end of the probe). This increased collection efficiency occurs because the far end of the probe has access to an electron population that has not been depleted by the presence of a collector running through it. This population increases the collection efficiency near the end of the probe and, at low density, causes the characteristics to approach that of a sphere, which is linear with respect to V. At higher densities, where the Debye length is small compared to the probe length, the volt-ampere curves look more like that of an infinite cylinder. A compromise that we have adopted to simplify the data processing is to assume an intermediate voltage dependence of $(eV/kT_e)^{3/4}$ in equation 1. Since this approximation does not rigorous correct for the end effect, the N_e measurements tend to be less accurate than the N_i measurements, except in regions of low density where photoemission causes significant N_i error, as discussed next.

The N_i Measurements

As indicated in Figure 2, N_i is derived from the ion saturation current which is described by Equation 2 for the case where the probe axis is perpendicular to the ion velocity vector (Hoegy and Wharton, 1973).

$$I_i = A\, N_i\, q_i\, v_i\, \pi^{-1}\, (1+kT_i/m_i v_i^2 + 2eV/m_i v_i^2)^{1/2} \quad (2)$$

where:

- q_i = ion charge
- v_i = ion drift velocity in the spacecraft rest frame
- T_i = ion temperature
- m_i = mean ion mass
- V = probe potential relative to the plasma

I_i consists of 3 components involving 1, kT_i and V whose physical analogs are illustrated in Figure 3. The first term (illustrated by the left panel) is typically an order of magnitude larger than the others, at least in the E and F-regions where m_i is large. It represents the ion current that is produced by ions being swept out by the side of the collector as it moves through the plasma at 8 to 9 km s^{-1}. These ions would be collected even if they had zero thermal velocity and if no attracting voltage were applied to the probe. The second term (middle panel) is the component of I_i produced by the ion thermal motion at temperature T_i. The third term (right panel) represents the additional ions that are attracted to the probe because of its accelerating potential, V.

For ease of data processing, N_i is usually derived by assuming that m_i=16, T_i=T_e, and v_i=v_s, where v_s is the spacecraft velocity. These simplifying assumptions are appropriate because of the dominance of the first term in the higher density regions of the ionosphere where Equation 2 is employed.

Notice that the slope of the ion saturation region (dI_i/dV) contains information on m_i, as illustrated in Figure 4 (Brace et al. 1973). Since dI_i/dV increases greatly when m_i falls below 10 or so, Brace et al. suggested that it could be used as a measure of m_i in the upper F-region and plasmasphere where the concentrations of H^+ and He^+ approach or exceed that of O^+. More importantly, however, dI_i/dV can be used to reject N_i values taken in regions where the m_i=16 assumption is invalid because of the presence of light ions. In practice, the switch-over from N_i to N_e has already occurred by the time the density is low enough for the ion mass assumption to matter. The switch-over criterion is discussed further in the section on Assessing the Measurement Accuracy.

The T_e Measurements

T_e is derived from the Langmuir equation for the electron retarding region given by

$$I_e = A\, N_e\, e\, (kT_e/2\pi m_e)^{1/2} \exp(eV/kT_e), \qquad (3)$$

which applies to probes of any geometry. The T_e measurement relies on the fact that the exponential term involves only two variables, T_e and V. The sensitivity of the method to T_e variations is illustrated in Figure 5, which shows theoretical volt-ampere curves for temperatures of 300 K, 1200 K and 4800 K, respectively. The effect of increasing T_e is to increase the amount of retarding potential that is required to cut off the thermal electrons and thus to achieve ion saturation. T_e is derived by fitting the volt-ampere curves using a linear approximation to the ion region and an exponential representation of the electron retardation region. Note that knowledge of the constants ahead of the exponential is not required to obtain T_e because only dV/dt and T_e affect the shape of the retarding region, and dV/dt is the known voltage sweep rate.

ACCESSING THE MEASUREMENT ACCURACY

If the sources of error described later in the Implementation section have been dealt with successfully the accuracy of the LP measurements should be better than 10%, and perhaps better than 5% for T_e. The precision of the density measurements, however, can be much greater, depending on the number of bits employed in the telemetry words, the electrometer noise level, and interference from other spacecraft systems. Relative accuracy of greater than 1% is typical.

One can assess the accuracy that has been achieved in a number of ways, including; (1) examining the internal consistency between LP theory and the shapes and amplitudes of the measured volt-ampere curves, (2) comparing the measurements by different probes on the same rocket or satellite, (3) comparing the probe measurements with those made by incoherent radars during overflights. Details of this approach and the results of past assessments are outlined below.

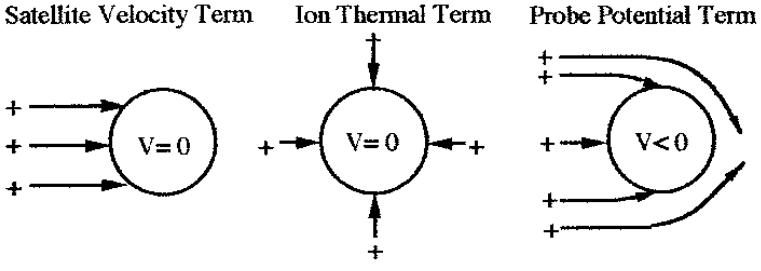

Figure 3. A sketch showing the physical origin of the three components of I_i represented in Equation 2; (1) ions that are swept out by the side of the collector moving at satellite velocity, (2) additional ions that reach the probe through their own thermal motion, and (3) ions that are attracted to the probe by its accelerating potential.

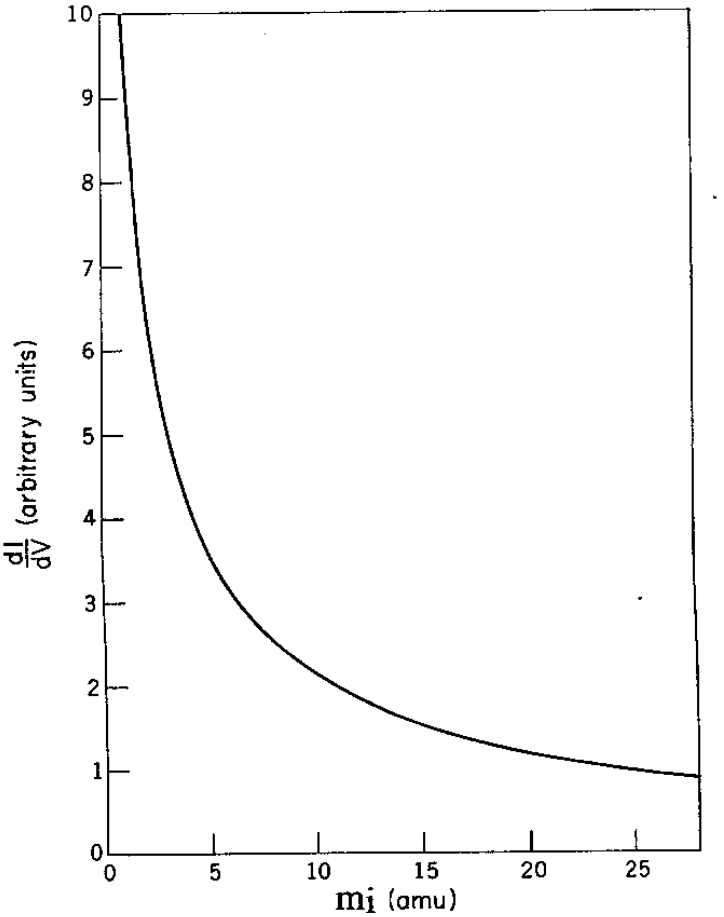

Figure 4. The effect of m_i on the slope of the ion saturation region, dI_i/dV. The slope is small in the E and F-regions where heavy ions dominate (m_i=16-32), so a precise knowledge of m_i is not required to obtain N_i. dI_i/dV is much larger in the plasmasphere where H^+ and He^+ ions dominate and the N_i measurements are subject to greater error. From Brace et al. (1973).

Internal Consistency Checks

The simple exponential relationship between T_e and I_e indicated in Equation 3 provides a powerful test of the validity of the T_e measurements. If the retarding region is not actually exponential, the measurement can be assumed to be invalid. The quality of fit can be used to detect such curves, and they should be discarded. Brace et al. (1971) showed that the ISIS-1 probes exhibited retarding regions

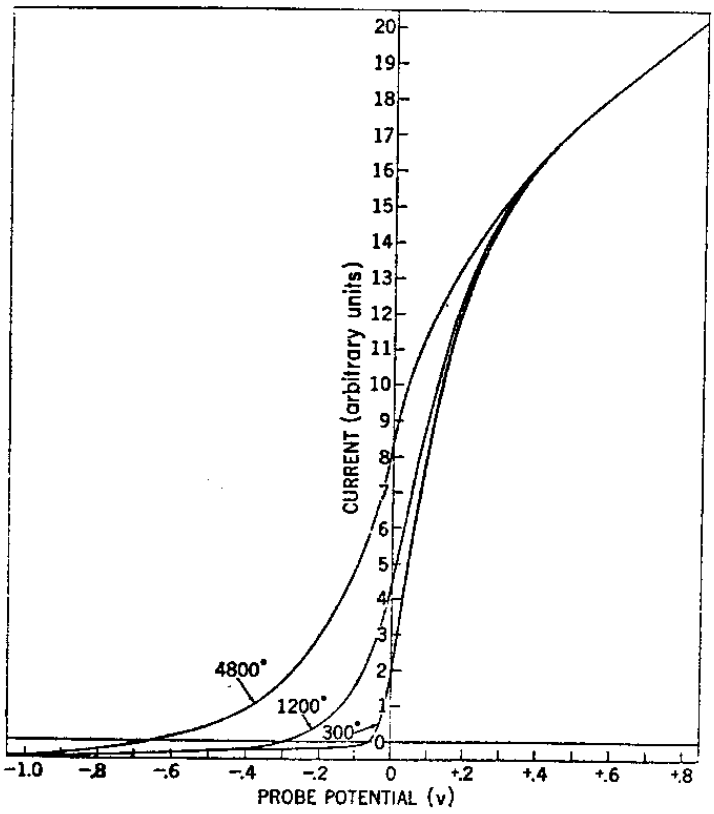

Figure 5. The effect of T_e on the volt-ampere curve. The main effect of T_e is to change the amount of retarding potential required to cut off the thermal electrons. From Brace et al. (1973)

that were exponential over a range of 6 or 7 kT_e. Typical electronic resolution of the volt-ampere curves allows T_e to be measured with an accuracy of better than 5%, except perhaps at very low density ($N_e<10^2 cm^{-3}$) where background currents due to photo emission may introduce errors. In darkness, T_e can be measured to much lower densities depending largely on the boom length and success in reducing background electrical noise from other spacecraft subsystems. Surface contamination of the collector may also introduce T_e errors, as discussed in the Implementation section.

The accuracy of the N_e and N_i measurements is typically of the order of 10% after corrections of N_e for certain systematic errors. Errors can be detected and assessed most readily by comparing the N_e and N_i measurements from the same volt-ampere curve. N_e and N_i are independently measured because they come from different regions of the volt-ampere curve using independent current collection theories. Since plasma neutrality requires N_e to equal N_i, we are free to use either as a measure of the density. The N_e measurements extend to lower densities because the electron saturation current is about a factor of 50 greater than the ion saturation current for the same density. As noted above, the inherent accuracy of the N_e measurements is limited by our understanding of the electron end effect which can introduce errors of up to a factor of 2 when short probes are used. The N_i measurements are more accurate, at least in the F-region, because the ion saturation current is almost exclusively due to the sweeping up of heavy ions by the known cross sectional area of the probe. At low densities ($N_i<<10^4 cm^{-3}$) photo emission from the probe introduces an error in the N_i measurements when the collector is in sunlight because it adds to the net I_i and produces an overestimate of N_i. Removal of the photo current during the analysis can extend the N_i measurements down to densities of the order of $1x10^3 cm^{-3}$. The presence of light ions (H^+ and He^+) can cause a similarly large overestimate of N_i if one fails to note their presence in the dI_i/dV.

Because the sources of N_e and N_i error differ, it is not surprising that they exhibit systematic differences where their dynamic ranges overlap (typically 10^3-$10^6 cm^{-3}$). Such differences arise from deliberate compromises between the requirements for the T_e and the density measurements, as described in the Implementation section. The short probes used for improved T_e accuracy on AE, DE-2 and PVO had large electron end effects, so the N_e values obtained using Equation 1 were systematically high by approximately 20%. The ion end effect (at 90° angle of attack) is far less important than the electron end effect, so the N_i values are more accurate. Our approach has been to apply an empirically derived normalization factor to the N_e values based on the N_e/N_i ratio measured in regions of higher density ($\sim 10^5$-$10^6 cm^{-3}$) where N_i is most accurate because the assumptions used in applying Equation 2 hold; i.e., the ion thermal motion contributes negligibly to I_i. After normalization, the N_e measurements are then employed at higher altitudes (lower densities) where the N_i measurements lose accuracy as uncertainties in m_i increase and photoelectron emission current from the probe becomes comparable to I_i. The photoemission current represents an effective I_i that is approximately equal to the true I_i at densities of the order of $1x10^4 cm^{-3}$ at the Earth-Sun distance. An empirically derived correction for the photo current extends the N_i measurements down to about $1x10^3$ cm^{-3}. No photoelectron correction is required in darkness, where N_i can be measured down to a value that is limited by the sensitivity of the electrometer and the resolution of the electrometer and the telemetry words. Typical systems place this limit around $1x10^2 cm^{-3}$. The lower limit on the N_e measurements is between 1 and 10 cm^{-3}, depending on the length of the boom and whether the spacecraft is in sunlight, and where the probe is mounted relative to sunlit surfaces of the spacecraft. While the normalization procedure removes the independence of the N_e and N_i measurements, it also removes the discontinuity in the

density measurements at the point of switch-over from N_i to N_e. The switch-over is usually set at about $2x10^4$ cm^{-3}.

Comparisons With Other In Situ Measurements

Comparisons between the measurements of two independent LPs on the same rocket or satellite may identify additional measurement errors that do not show up in the internal consistency checks. Systematic differences may arise from mechanical failure, surface contamination of one or both probes, or differences in mounting location. In the late 60s, multiple long-wire probes were flown on the same rocket to see if the type of metal coating on the collector had any affect upon the T_e measurements (Brace et al., 1971). They found good agreement in the T_e measurements made by long-wire probes made of different metals or having different surface coatings.

A later rocket flight at Wallops Island was timed to coincide with an overflight of Atmosphere Explorer 17 which carried the same type of long-wire stainless steel probes that were carried on the rocket. In these early days of satellites, it had been feared that the high speed of the satellite might in some unspecified way affect the T_e measurements. The excellent agreement between the rocket and satellite measurements put that question to rest (Brace et al., 1971).

Comparisons among the measurements by different types of plasma instruments on the same satellites offered other insights into the validity of the various techniques. Donley et al. (1969) found good agreement among the measurements made by the cylindrical and planar LPs and the planar retarding potential analyzers on the Explorer 31 satellite. Findlay and Brace (1969) found excellent agreement when comparing measurements from identical LPs on physically quite different satellites (Explorer 31 and Alouette II) while they were orbiting in close proximity. Miller et al. (1984) also found very good agreement between the measurements of N_e, N_i, and T_e made by the Langmuir probe and the retarding potential analyzer on the PVO spacecraft.

Comparisons with Ground-based Techniques

In 1968, two rockets were launched near the Arecibo radar facility in Puerto Rico to allow comparisons of LP and incoherent scatter measurements. Brace et al. (1969) reported that the daytime T_e measurements were in excellent agreement with the radar measurements, but the probe temperatures were slightly higher on the nighttime flight. The T_e measurements by a platinum and a stainless steel probe on the nighttime flight disagreed by 10%; a difference that was not present in the daytime measurements. The inherently large surface patchiness of the stainless steel probe may have led to the slightly higher values of T_e from that probe.

More extensive incoherent radar and LP comparisons were reported by McClure et al.(1973) based on overflights of OGO-6. The long-wire LP measurements from OGO-6 yielded T_e values about 15% higher than the radar measurements (McClure et al., 1973). Much better agreement was reported by Benson et al. (1977) who compared AE-C short probe measurements with those made simultaneously by the Millstone Hill, Chatanika, St. Santin, and Arecibo radars. The single disagreement was at Millstone Hill where the radar T_e measurements were lower than the probe measurements by an average of 11%. These comparisons were valuable because they uncovered a systematic difference between the radar measurements from Millstone and the other locations. The generally better T_e agreement between the radars and the short probes suggests that the accuracy of the earlier long probe measurements may have suffered from a combination of surface patchiness and geomagnetically induced potentials, both of which cause energy smearing of the electron retardation regions at very low T_e. These effect are described in the Implementation section.

While these comparisons among in situ and remote measurements have demonstrated the validity of the LP technique in a wide variety of space applications, they do not obviate the need to avoid implementation errors in any new mission. Some sources of measurement error are outlined below.

IMPLEMENTATION ISSUES

A number of factors are critical for successful Langmuir probe measurements; (1) proper sensor placement, (2) reduction of collector work function patchiness, (3) reduction of collector surface contamination, (4) limitation of geomagnetically induced potentials in the collector, (5) adequate resolution and recovery of the volt-ampere curves, and (6) attention to spacecraft design details. If these factors are not dealt which successfully the full measurement accuracy that is afforded by the LP theory will not be achieved. Inattention to some of these items can preclude the measurements completely, especially for T_e.

Boom and Sensor

The use of a boom is required to assure that the probe is placed in the undisturbed plasma; i.e., beyond the spacecraft sheath and outside the spacecraft wake, as shown earlier in Figure 1. To achieve this goal a boom length of between 30 and 100 cm is usually adequate in the ionosphere. Longer booms may require hold-down devices to prevent damage during launch. Two independent sensors are usually required, particularly on a spinning satellite, to assure that at least one probe is in the undisturbed plasma at all times. Figure 6 shows the design of the probes used on DE-2 and PVO. A solid triaxial rod served as the boom. The triax

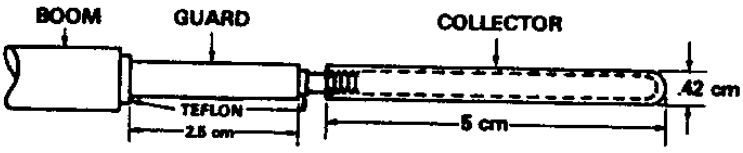

Figure 6. Details of the sensor design used in the DE-2 and PVO Langmuir probes. The collector is threaded onto the inner rod of a solid triax that serves as the boom. The outer sheath is trimmed back a few cm to expose the inner sheath which serves as a guard element. The 3 boom elements are insulated from each other by Teflon sleeving. From Krehbiel et al. (1980).

was manufactured using a titanium central rod and two concentric titanium sleeves, all insulated from each other by Teflon spaghetti. The boom construction involved an extrusion process which provided an electrical connection to the probe that was essentially free of the microphonic noise that had plagued the AE probe measurements at very low densities. The use of titanium provided the necessary combination of mechanical strength and low weight. The end of the central rod was threaded to permit the collector to be screwed on at the final opportunity prior to launch, using a metal epoxy adhesive to keep the collector from coming off during launch. The guard electrode was formed by simply exposing a few centimeters of the metal inner sheath. Ideally, the guard should be longer than a few centimeters, but this would have decreased the spacecraft-to-probe area ratio, a factor whose importance is discussed in the section on Spacecraft Design Factors. The thickness of the outer metal sheath was selected to provide sufficient strength to withstand the vibration and acceleration loads of the launch.

Collector Surfaces

Work function patchiness can be a significant source of error in the T_e measurements, especially in regions of very low temperature where the electrical patchiness of a normal (polycrystalline) collector approaches or exceeds the mean thermal energy of the electrons. A patchiness of $1kT_e$ means that the first kT_e of the retarding region will be smeared out because some parts of the probe are positive while other parts are still in the retarding region. If the patchiness is much larger than a kT_e, the retarding region may be "energy smeared" enough to preclude an accurate measurement of T_e. A polycrystalline probe can easily have a built-in patchiness exceeding 100 mV, which corresponds to a voltage equivalent of 1 kT_e at 1160 K. Such a probe will produce serious T_e errors at E-region temperatures (~300 K) where the first 3 or 4 kT_e of the electron energy distribution will be smeared out. The higher temperatures of the F-region (~2000 K) would still be measured accurately because only the lowest kT_e would be affected by the patchiness. In practice, energy smearing can be detected by examining the amplitude of the electron current at the inflection point, V_p, shown in Figure 2. If the surface patchiness is small, I_e at V_p should be consistent with the random electron flux, $N_e e(kT_e/2\pi m_e)^{1/2}$.

The thin-wire probes used on the early satellites were made of stainless steel, so they undoubtedly had this problem to one degree or another. These satellites orbited at high altitudes, however, where T_e generally exceeded 1000 K. Enough of the retarding region remains at these temperatures to allow a good fit for T_e. Patchiness affects the N_e and N_i measurements only to the extent that the inflection point occurs too early, and V_p is incorrectly identified. The resulting density error is minor, however, because a 100 mv uncertainty in V is not significant in the electron and ion saturation regions where the current varies only weakly with probe voltage.

Work function patchiness has been reduced in later applications by the use of either vitreous carbon probes (M. Bujor, 1973) or by using probes having highly oriented metal crystal surfaces (Brace et al., 1973). The latter solution was based on the work of Weissman and Kinter (1963) who employed a chemical vapor deposition process to produce cathodes having surface potentials that were uniform within 5 mv. This technology was employed to make the cylindrical probes used on the AE missions which were designed to dive deeply into the E-region where patchiness would have caused important errors in the T_e measurements. Collectors of the same type were used later on the DE-2 and PVO spacecraft. Figure 7 shows a photographic cross section of one of the rhenium collectors used on PVO. The probe diameter was 0.42 centimeter including a 1 mm layer of highly oriented rhenium crystals. A second probe, used for redundancy in these missions, had highly oriented molybdenum surfaces. This approach appears to have been very successful, since both probes were able to measure T_e down to temperatures of 300 K on the AE-C and PVO missions. DE-2 had a 300x1000 km orbit, so it did not experience regions of very low T_e.

Probe Contamination

Surface contamination can produce its own type of patchiness even when the potential of the underlying probe is highly uniform. While the collectors are cleaned prior to launch, they can be recontaminated during the launch phase or by outgassing from the spacecraft after orbit has been achieved. The contaminating material then experiences chemical changes under the action of solar EUV radiation and exposure to thermospheric atomic oxygen. If the contaminating layer is a poor conductor and is not uniformly distributed, different areas of the surface may charge to different potentials, thus producing energy smearing of the electron retarding region which introduces error into the T_e calculation. Surface contamination has its

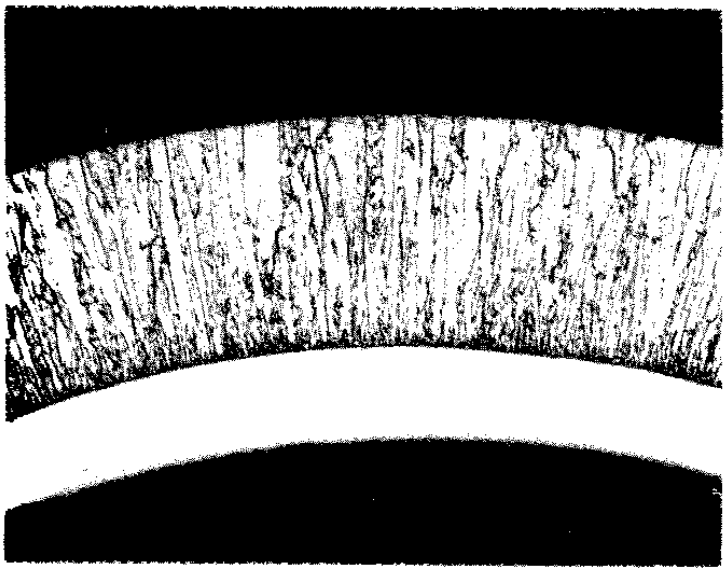

Figure 7. Magnified photographic cross section of a collector (x250) showing the radial alignment of the crystals that form its surface. This type of surface has a work function patchiness of less than 5 mV., essentially eliminating energy smearing of the electron retardation region.

greatest effect at high densities because the larger currents produce larger voltage drops across the insulating surface layers. While the voltage drop may be smaller at low densities, the discharge time of the insulating layer will be longer because the ion and electron fluxes from the ionosphere are lower. This effect can be seen as an exponential discharge signature in I_i at the beginning of the ion saturation region immediately following the retrace of the sawtooth sweep (from positive to negative). Such signatures were observed in curves from the AE-E probes later in that mission. The use of redundant LP sensors makes it easier to detected the presence of surface contamination, since the different probe locations may lead to different degrees of contamination and different delays in their onset. Our experience with the AE, DE and PVO probes suggests that rhenium surfaces may be more susceptible to contamination than molybdenum surfaces, but this conclusion is based on poor statistics.

Inflight Cleaning

In anticipation of the possibility of contamination the AE-C, D and E probes were designed to be heated by internal filaments. Owing to effectiveness of radiation to space, however, the available electrical power was insufficient to achieve and maintain effective bake-out temperatures (>300° C). One of the AE-C collectors developed symptoms of contamination about 6 weeks after launch, while the other remained free of contamination throughout the 5-year mission. Both of the collectors on AE-D and E eventually became contaminated to some degree, and internal heating was ineffective in improving the quality of the volt-ampere curves. Eventually these probes became useful only for measuring N_i which does not appear to be affected by contamination, perhaps owing to the high velocity of the ions in the spacecraft reference frame.

The contamination experienced in the AE missions led us to try an alternative cleaning technique in the DE-2 mission; i.e., using ionospheric electrons to bombard the probe surfaces. The cleaning was achieved by applying +150V to one of the probes as the spacecraft traversed the denser parts of the ionosphere (Krehbiel et al., 1981). This method is simpler than internal heating and requires less power. It is also faster and apparently more effective. The probe was cleaned about 6 days into the mission by electron bombardment for a full orbit. No evidence of contamination had been evident in the volt-ampere curves before the cleaning procedure was conducted, and the cleaning did not appear to affect the quality of the volt-ampere curves. The probe was cleaned again 18 month later just before the end of the mission, and again no evidence of contamination was observed before or after the cleaning. The volt-ampere curves from the other DE-2 probe, which could not be cleaned, began to show evidence of contamination several weeks after launch, and its effects were evident throughout the remainder of the mission. These results have led us to conclude that both probes had become contaminated prior to or during the launch, but that the effects did not show up immediately. The initial cleaning of the first probe apparently was successful in removing the contamination before exposure to solar EUV and to chemically active atoms (O and O^+) began to reduce the conductivity of the contaminating layer. The fact that the first probe remained uncontaminated throughout the mission suggests that the second cleaning procedure was unnecessary. From this limited experience we have concluded that electron bombardment should be used early in the mission to clean the probes before they have experienced extended exposure to the space environment.

Inflight cleaning was not necessary in the PVO mission because solar wind ions (~1 keV protons) bombarded the spacecraft for at least 95% of its 24 hour orbit. Neither of the LP collectors became contaminated during the 14-year mission. One might expect similar ion and electron sputtering to occur in high inclination Earth orbits which encounter energetic ions and electrons at high latitudes. This kind of natural inflight cleaning could account for the absence of LP contamination in the early missions which were not deep-divers (Tiros-7, Explorers 17, 22, 23, 31, 32, Alouette-II, ISIS-1, and ISIS-2).

Magnetically Induced Potentials

When the spacecraft moves at high velocity, **v**, through the geomagnetic field, **B**, a potential gradient of the order

of 300 mv/m is induced in the collector. For a collector of length, l, the potential is **B**x**v**.l. The resulting potential gradient produces the same kind of energy smearing that is caused by surface contamination or by the inherent patichness of polycrystalline probe surfaces.

The solution to the energy smearing problem has been to use short probes (as in AE, DE and PVO) or to keep the probe aligned with **B** or **v**. Alignment with **v** is not desirable because this enhances the ion end effect (Brace et al., 1973) which makes the volt-ampere curves more difficult to interpret.

Alignment with **B** is sometimes feasible. The Explorer 22 and 23 spacecraft were magnetically stabilized such that the long-wire probes were aligned with the geomagnetic field throughout the orbit, thus eliminating the voltage induced in the collector. The spacecraft used in later missions did not offer this capability, so short probes were employed as soon as their advantage for low T_e measurements became obvious. The voltage induced in the AE and DE short probes introduced a maximum energy smearing of 15 mV, which corresponds to about $1kT_e$ at 150 K. Thus, the use of short probes essentially removed the low temperature limit although it may have enhanced the errors in the N_e measurement due to the electron end effects discussed earlier. **B**x**v** effects are unimportant for missions to unmagnetized planets like Mars and Venus, but the use of highly oriented probe surfaces and inflight cleaning remains important because T_e can be much lower in certain regions of the ionospheres of these planets.

The Electronics

Different orbits and scientific objectives may place different requirements on the electronics. The pertinent questions to be addressed are; (1) What ranges of N_e and T_e are likely to be encountered in the selected orbit and at the level of solar activity expected during the mission?, (2) Does the mission science require the full range of N_e and T_e to be measured, or is it possible to focus on narrower ranges of altitude, latitude or local time?, (3) Is the spacecraft spin-stabilized or 3-axis stabilized?, (4) What sweep repetition rate is consistent with the spacecraft spin rate, the desired spatial resolution, and the available telemetry rate?, (5) How many sensors are to be operated, and where should they be mounted to avoid or minimize spacecraft wake and sheath effects?, (6) Should each probe system be fully redundant to permit simultaneous measurements, or can the probes time-share one electrometer and sweep generator?, (7) Is the available data rate adequate to permit the volt-ampere curves themselves to be recovered, or will some form of electronic inflight processing be required to obtain the desired spatial resolution along the orbit?, (8) Is inflight cleaning of the collectors likely to be required?, (9) Will the proposed spacecraft provide normal V_S, or will design changes be required? The answers to these questions will affect the design of the electronics, as discussed below.

The task of the electronics is to apply the desired range of V_a to the probe(s) and to measure the resulting currents. If the full range of N_e in the ionosphere (5 to 6 orders of magnitude) is to be measured, the electrometer must have a wide dynamic range. T_e typically varies by a factor of 30; from about 300 K in the E-region to greater than 10,000 K in the upper F-region at high latitudes. Since the width of the retarding region is proportional to T_e, a single sweep amplitude will not be adequate in most missions. If the sweep amplitude is high enough to reach full ion saturation at high T_e the retarding region will be crossed too quickly at low T_e to be followed by the electrometer or to be resolved at realistic telemetry sampling rates.

The early exploratory missions (prior to 1970) addressed this problem in a primitive way by sequencing through 2 voltage sweep amplitudes and 4 electrometer ranges. This approach seriously limited the spatial resolution of the measurements because the gain and sweep amplitude were seldom optimum. To improve the curve resolution more recent LPs (AE, DE-2, PVO) employed adaptive circuitry which automatically set the electrometer gain and sweep amplitude so as to focus on the portion of the volt-ampere curve actually used to determine N_i, N_e and T_e. This system was described by Brace et al. (1973) for the AE probes and by Krehbiel et al. (1980, 1981) for the PVO and DE-2 instruments. The approach involved a concept called curve framing in which the electrometer gain and sweep amplitude are continuously adjusted to produce the same "ideal curve" at the output of the electrometer over a wide range of N_e and T_e variations. The process is analogous to the laboratory situation in which one continually adjusts the vertical gain and horizontal frequency of an oscilloscope to frame a waveform whose amplitude and frequency are changing.

The adaptive circuitry adjusts the electrometer gain using the ion current level observed at the beginning of each sweep. This assures that the ion saturation region is ideally resolved. The gain is then locked and the sweep is begun to generate a volt-ampere curve. Level detectors and time counters examine the retarding region to obtain an approximate value of kT_e for use in setting up the amplitude and start voltage to be used on the following sweep. The algorithm that is used in the framing process produces a start voltage and sweep amplitude that covers just enough of the ion and electron saturation regions to permit the geophysical parameters to be derived; i.e., the portions illustrated earlier in Figure 2. The sweep amplitude ranges from about 300 mV to 10 V, corresponding to a T_e variation from about 300 K to 10,000 K. The correct gain setting for the I_i measurement will cause I_e to go above full scale toward the end of the

sweep. When this occurs the electrometer is down-ranged immediately by a factor of 10 to resolve the rest of the electron saturation region. When the curve-framing process breaks down due to such factors as discontinuous jumps in V_S or small-scale structure in N_e, a large amplitude fault sweep is introduced to allow the system to reconverge.

Finally, the adaptive process generates gain and sweep amplitude settings that are surrogates of the N_i and T_e variations that they are tracking, and they can be recovered using a far lower telemetry rate than is required to recover the volt-ampere curves themselves. Since the sweep amplitude is no greater than is required, the curve framing process also permits the sweep repetition rate to be increased or the telemetry rate reduced. This is particularly important in planetary missions where the telemetry rate may be very low. The electronics must also be able to sample and store occasional volt-ampere curves for later recovery, since this simple inflight processing scheme requires calibration via more sophisticated curve analysis on the ground.

Spacecraft Design Factors

Since the LP sweep voltage is applied with respect to the spacecraft potential reference, the spacecraft design should be examined to see if it includes any features that might affect V_S which should remain low and stable. Historically, the most common spacecraft potential problems are caused by; (1) exposed metal connecting tabs on the solar arrays, and (2) insufficient external conducting area to return the LP current to the ionosphere without causing excessive changes in V_S. Since the net current to the spacecraft-probe system must be zero, increases in I_e to the probes must be offset by identical reductions in I_e flowing to the spacecraft. The spacecraft design should support such I_e changes without significant changes in V_S. Such changes subtract from the voltage that actually reaches the probe and can interfere with measurements made by other instruments which are referenced to Vs.

The achievement of a stable V_S requires an external conducting area that is several hundred times larger than the combined probe and guard areas. This conducting area must not be in the wake of the satellite because neither the ions or electrons have access to those surfaces (Samir et al., 1979). Although the total external area of the spacecraft is typically more than 10,000 times that of a LP, most of this area will be nonconducting. Bare metal surfaces tend to have absorptivity and emissivity coefficients that conflict with spacecraft thermal design requirements. This conflict can usually be resolved by painting some of the exposed spacecraft surfaces with a conductive thermal paint, or by adding conductive surfaces elsewhere. Some spacecraft provide the required area ratio by employing conductive coatings over glass plates that cover the solar cells. When an adequate area ratio is not achievable in these ways, it may be necessary accept a smaller area ratio. In this situation one might avoid using the LPs in the electron saturation regions where they collect the largest current. In this case, only T_e and N_i measurements are possible. This approach was used in the AE missions to reduce possible interference with the retarding potential analyzers and the ion mass spectrometers.

We have seen several cases of unusually high V_S. They all have all been traced to the use of negative grounded solar arrays whose interconnecting metal tabs were exposed to the plasma. These tabs have voltages that range from 0 to about +40 volts with respect to the spacecraft, so they act like an array of small Langmuir probes that collectively attempt to draw a larger electron current than the rest of the spacecraft is able to return to the ionosphere. To maintain zero net current to the system, V_S shifts sufficiently negative to drop the array electron current to sustainable levels. Such high negative potentials (~30-40 V) usually preclude the T_e and N_e measurements, since the available range of V_a is insufficient to drive the probe out of ion saturation. This problem is limited to the parts of the orbit where the spacecraft is sunlit

Two solutions to the solar array problem have been found successful. The first involves grounding the positive end of the solar array thus exposing only negative potentials to the plasma. While the array draws an enhanced ion current, this current is easily balanced by a slight decrease in V_S to draw the required additional electron current to the spacecraft. The Explorer 22, 23, Tiros, AE and DE spacecraft used such negative arrays, and they experienced normal ranges of V_S. Alouette-II, ISIS-1, OGO-6, ISIS-2, and PVO had positive arrays. The problem was solved by painting the solar cell tabs with silicon rubber to keep them from drawing electrons from the plasma. This was a simple, effective and low cost fix.

SUMMARY AND CONCLUSIONS

In this paper we have discussed the Langmuir probe method and various ways to improve measurement accuracy. Many years of experience indicates that the accuracy of the measurements depends on the details of the implementation. The factors most critical to success involve; (1) using a relatively short probe that has inherently low surface patchiness and that can be cleaned very early in the mission by electron or ion bombardment, (2) mounting the probe on a boom that is long enough to place the collector in the undisturbed plasma that lies beyond the spacecraft ion sheath, (3) using adaptive circuitry in the electronics to resolve the volt-ampere curves over a wide range of N_e and T_e and to facilitate the recovery of some of the curves for ground analysis and verification, (4) designing the spacecraft to have an adequate

conducting area and a solar array that does not cause V_S to be excessively negative.

The degree of success actually achieved can be determined by a series of internal consistency tests. First, the volt-ampere curves should exhibit the form indicated by the theory. The ion saturation regions should be approximately linear and have a slope that is consistent with the known mean ion mass in the region. The electron saturation region should exhibit the expected voltage dependence. The electron retarding region should be truly exponential over several kT_e. The amount of current at the inflection point (V_p) should be consistent with the random electron current. The N_e measurements should be consistent with the N_i measurements at densities where the two techniques overlap, recognizing that end effects will tend to cause N_e to be slightly higher than N_i. No hysteresis should be evident in the curves when the probe voltage is swept in opposite directions, and no time constants should be evident in I_i immediately following the sweep retrace. These criteria for internal consistency are very demanding and, if met, one can have a high degree of confidence in the measurements.

We also have reviewed a number of comparisons among LP measurements and with the measurements from other instruments on the same spacecraft. Additional confidence has been achieved by comparing the LP results with ground based measurements made during overflights of incoherent scatter facilities. We have concluded that Langmuir probes can provide accurate ionosphere measure-ments if several important implementation challenges are addressed successfully.

Acknowledgements The excellent engineering efforts of many people have led to the success of the LP experiments referenced in this paper. To mention just a few of them specifically; George R. Carignan at the University of Michigan directly supervised the design and construction of the rocket and satellite electronics and personally built the thin-wire probes, James A. Findlay, formerly at Goddard Spaceflight Center, was the Experiment Engineer on the early missions, and John P. Krehbiel, now at NASA Headquarters, was the Experiment Engineer for the LPs on AE, DE and PVO. The programming work of Bob Theis at Goddard was indispensable in the development of codes for fitting the volt-ampere curves and for processing the masses of data that were generated during these missions.

REFERENCES

Benson, R. F., P. Bauer, L. H. Brace, H. C. Carlson, J. Hagen, W. B. Hanson, W. R. Hoegy, M. R. Torr, R. H. Wand and V. B. Wickwar, Electron and ion temperatures - A comparison of ground based incoherent scatter and AE-C measurements, *J. Geophys. Res., 82*, 36, 1977.

Boggess, R. L., L. H. Brace and N. W. Spencer, Langmuir probe measurements in the ionosphere, J. *Geophys. Res., 64*, 1627, 1959.

Brace, L. H., N. W. Spencer and A. Dalgarno, Detailed behavior of the mid-latitude ionosphere from the Explorer 17 satellite, *Planet. Space Sci., 13*, 647, 1965a.

Brace, L .H., and B. M. Reddy, Early electrostatic probe results from Explorer 22, *J. Geophys. Res., 70*, 5783, 1965b.

Brace, L. H., and J. A. Findlay, Comparison of cylindrical electrostatic probe measurements on Alouette II and Explorer 31 satellites, *Proc. IEEE, 57*, 1057, 1969.

Brace, L. H., H. C. Carlson and K. K. Mahajan, Radar backscatter and rocket probe measurements of electron temperature over Arecibo, J. *Geophys. Res., 74*, 1883, 1969.

Brace, L. H., G. R. Carignan and J. A Findlay, Evaluation of ionospheric electron temperature measurements by cylindrical probes, *Space Res., 11*, 1079, 1971.

Brace, L. H., R. F. Theis and A. Dalgarno, The cylindrical electrostatic probes for Atmosphere Explorer- C, D and E, *Radio Science*, **8**, 341, 1973.

Brace, L. H., and R. F. Theis, The behavior of the plasmapause at midlatitudes: ISIS-I Langmuir probe measurements, J. *Geophys. Res., 79*, 1871, 1974.

Brace, L. H., and R. F. Theis, Global empirical models of ionospheric temperature in the upper F region and plasmasphere based on in situ measurements of the Atmosphere Explorer-C, ISIS-1 and ISIS-2 satellites, *JATP, 43*, 1317, 1981.

Brace, L. H., W. R. Hoegy, R. F. Theis, Solar Euv measurements at Venus based on photoelectron emission from the Pioneer Venus Langmuir probe, J. *Geophys. Res., 93*, 7282, 1988.

Bujor, M., Work function variation across the surface of tungsten and vitreous carbon, in *Photon and Particle Interactions with Surfaces in Space*, edited by R.J.L. Grard, 323, Reidel, Dordrecht, Holland, 1973.

Donley, J. L., L. H. Brace, J. A. Findlay, J. H. Hoffman, and G. L. Wrenn, Comparison of results of Explorer XXXI direct measurement probes, *Proc. IEEE, 57*, 1078, 1969.

Findlay, J., and L. H. Brace, Cylindrical electrostatic probes employed on Alouette II and Explorer 31 satellites, *Proc. IEEE, 57*, 1054, 1969.

Hoegy, W. R., and L. E. Wharton, Current to moving spherical and cylindrical electrostatic probes, *J. Appl. Phys., 44*, 12, 5365, 1973.

Krehbiel, J. P., L. H. Brace, and R. F. Theis, J. R. Cutler, W. H. Pinkus and R. B. Kaplan, Pioneer Venus Orbiter Electron Temperature Probe, *IEEE Trans. Geosci. Remote Sens.*, GE-18, No. 1, 49, 1980.

Krehbiel, J. P., L. H. Brace, R. F. Theis, W. H. Pinkus, and R. B. Kaplan, The Dynamics Explorer Langmuir probe instrument, *Space Science Instrumentation, 5*, 493, 1981.

Langmuir, I., and H. Mott-Smith, Jr., Studies of electric discharges in gas at low pressures, *Gen. Elec. Rev. 616*, Sept 1924.

McClure, J. P., W. B. Hanson, A. F. Nagy, R. J. Cicerone, L. H. Brace, M. Baron, P. Bauer, H. C. Carlson, J. V. Evans, G. N. Taylor and R. F. Woodman, Comparisons of T_e and T_i

from OGO-6 and from various incoherent scatter radars, *J. Geophys. Res.*, *78*, 197, 1973.

Miller, K. L., W. C. Knudsen, and K. Spenner, The dayside Venus ionosphere. I. Pioneer Venus retarding potential analyzer experimental observations, *Icarus*, *57*, 386, 1984.

Mott-Smith, J. M, and I. Langmuir, The theory of collectors in gaseous discharges, *Phys. Rev.*, *28*, 727, 1926.

Reddy, B. M., L. H. Brace and J. A. Findlay, The Ionosphere at 640 km on quiet and disturbed days, *J. Geophys. Res.*, *72*, 2709, 1967.

Samir, U.,, L. H. Brace, H. C. Brinton, About the influence of electron temperature and relative ion composition on the ion depletion in the wake of the AE-C satellite, *Geophys. Res. Lett.*, *6*, 101, 1979.

Spencer, N. W., L. H. Brace, G. R. Carignan, D. R. Taeusch and H. Niemann, Electron and molecular nitrogen temperature and density in the thermosphere, *J. Geophys. Res.*, *70*, 2665, 1965.

Weissman, I. and M. L. Kinter, Improved thermionic emitter using uniaxial oriented tungsten, *J. Appl. Phys.*, *34*, 3187, 1963.

Larry H. Brace, Space Physics Research Laboratory, The University of Michigan, 2455 Hayward, Ann Arbor, MI 48109